# THE INTERFACE BETWEEN EMPIRICAL AND SIMULATION-BASED GROUND-MOTION MODELS

GAIL M. ATKINSON

Western University, London, Canada

*gmatkinson@aol.com*

**Abstract**. Ground-motion models (GMMs) are a key driving component of PSHA results and their uncertainty. GMMs that bridge seismological and empirical approaches are an effective tool to represent the distribution of ground motion and its uncertainty in seismic hazard assessment. A methodology is presented that uses ground-motion data recorded on rock sites in eastern North America and shows how they can be used to calibrate simple scalable seismological models of ground motion generation and propagation. Such GMM models can directly account for the gross features of source scaling (magnitude and stress parameter), attenuation, site response and kappa effects. It is shown that by application of appropriate GMM strategies, sigma (aleatory uncertainty) could be greatly reduced for nuclear sites on rock, resulting in lower calculated hazard. This reduction in sigma requires that high-quality seismic monitoring (e.g. broadband seismograph stations) be installed and operated over a period of years, and an investment be made in data analysis and targeted GMM development using the data.

**Key Words**: ground motion models, empirical, uncertainty

## 1. INTRODUCTION

Ground motion models (GMMs), sometimes referred to as ground-motion prediction equations, are a key component in probabilistic seismic hazard analysis (PSHA), and often the most important uncertainty affecting the results of a PSHA. They provide median estimates of the ground-motion amplitudes as a function of explanatory variables such as magnitude, distance, and site conditions, along with estimates of variability. Empirical GMMs are commonly used in data-rich regions such as California and Japan. For instance, the second generation Pacific Earthquake Engineering Research–Next Generation Attenuation-West (NGA-W2) project [1] includes empirical GMMs for crustal earthquakes in active tectonic regions [2, 3, 4, 5, 6] and is widely used in practice (e.g. [7]). An alternative method, commonly-used in data-poor regions, is to derive a GMM using a simulation-based approach, in which a seismological model is calibrated with a set of empirical data. The advantage of such an approach is that robust magnitude and distance scaling behaviors can be imposed, whilst accommodating regional features that can be determined from limited available data. There are numerous examples of such simulation-based models in practice, including stochastic point-source models [8, 9, 10, 11] and finite-source stochastic and broadband simulations [12, 13, 14, 15, 16].

Yenier and Atkinson [17, 18] developed a regionally-adjustable generic GMM based on the concept of equivalent point-source simulations. They derived a robust simulation-based GMM that can be adjusted to different regions by modifying the input parameters (e.g. geometrical spreading, stress parameter, and calibration factor models), and examined the applicability of the model for earthquakes in California and central and eastern North America [18]. The parameters for the generic GMM were originally defined by calibrating a seismological model to match the empirical ground-motion amplitudes recorded in California [17]. Specifically, Yenier and Atkinson [17] used the rich California ground-motion database to define elements of the functional form and calibrate the overall model scaling behavior in magnitude and distance. They also determined the geometric spreading, anelastic attenuation and stress parameter models that describe ground-motions amplitudes for California. The model was parametrized in a way that isolates the effects of magnitude scaling, stress parameter scaling, geometrical spreading and anelastic attenuation on ground-motion amplitudes, so that the

approach can be readily transported to other regions by modifying just a few regional source and attenuation parameters. Figure 1 illustrates the YA15 (Yenier and Atkinson, 2015) equivalent point-source model GMM for California and active crustal regions (for B/C site conditions of 760 m/s), in comparison to the underlying NGA-W2 data used in model development. The generic GMM matches the data as well as strictly-empirical GMMs developed from the NGA-W2 database and has the added benefit of being parameterized by simple seismological parameters.

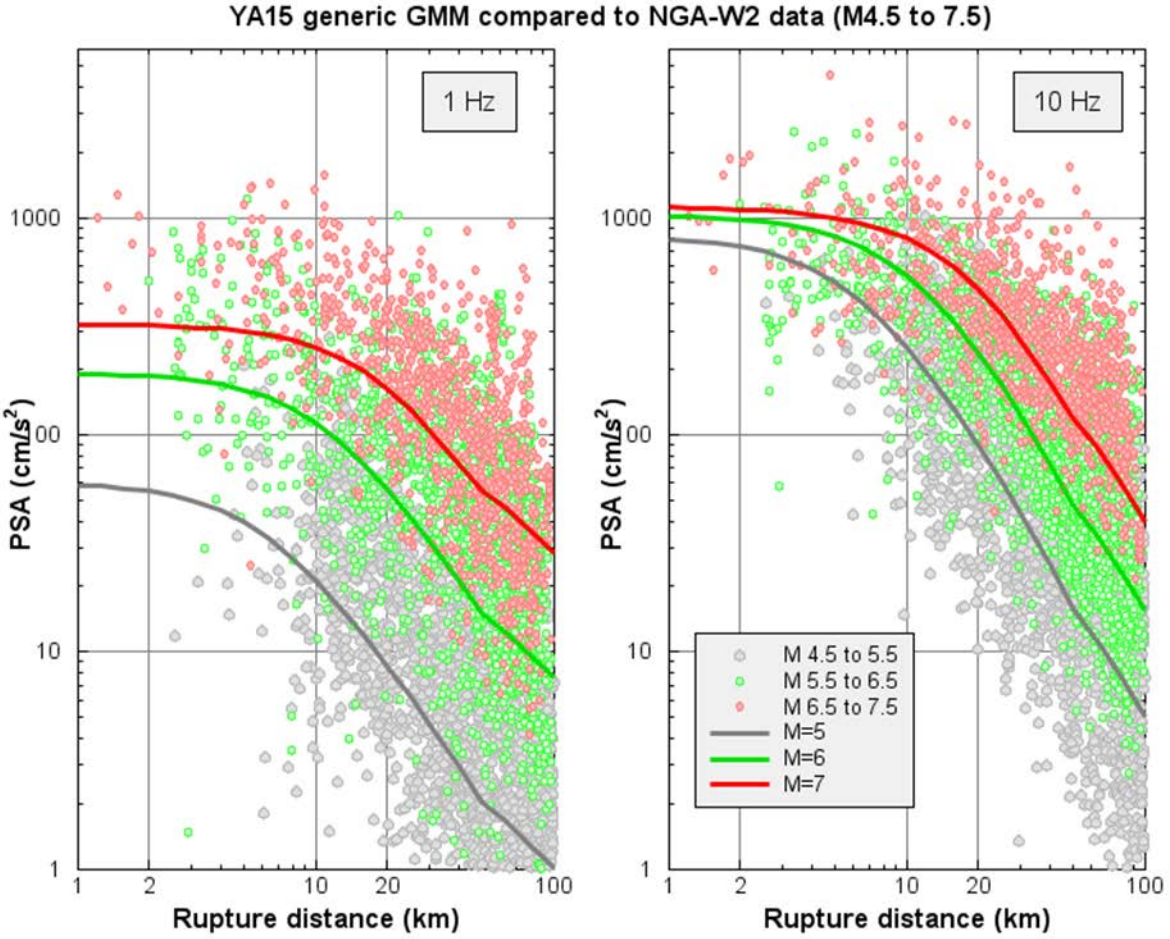


*FIG. 1. Comparison of YA15 generic GMM for B/C site conditions for crustal earthquakes in active regions, developed using equivalent point-source approach (lines) with ground-motion amplitudes of NGA-W2 database, corrected to equivalent values for B/C sites using the empirical site model of Seyhan and Stewart [19] (circles). Magnitude ranges are colour-coded.*

## 2. THE GENERIC GROUND-MOTION MODEL – A CALIBRATED EQUIVALENT POINT-SOURCE APPROACH

Atkinson et al. [20] used the generic equivalent point-source approach of Yenier and Atkinson (YA15, Fig. 1) to develop a GMM for ground motions on rock sites in eastern North America (ENA). The model can be written as follows, with model coefficients being provided in the appendix. The equation is used for the geometric mean horizontal component of motion.

$$\ln(Y) = F_M + F_Z + F_{\Delta\sigma} + \gamma \quad D_{rup} + F_S + C \tag{1}$$

where ln($Y$) is the logarithm (natural logs) of a ground-motion intensity measure, such as peak ground acceleration (PGA), velocity (PGV) and 5%-damped pseudo-spectral acceleration (PSA) at a selected oscillator frequency. $F_E$, $F_Z$, $F_\gamma$, and $F_S$ are the model components for earthquake source, geometrical spreading, anelastic attenuation, and site amplification, respectively. The $C$ term is an empirical constant that scales the simulation amplitudes to match the amplitude of the observations. The source ($F_E$) and geometrical spreading ($F_Z$) terms are constrained in their scaling behavior by the equivalent point-source simulations that were validated using the rich empirical database from California (e.g. Fig.1). Regional ground-motion data for ENA were inverted to determine the anelastic attenuation term ($F_\gamma$), site amplification model ($F_S$) and the calibration constant ($C$).

The source term ($F_E$) isolates the effects of magnitude and stress parameter on the ground-motion amplitudes:

$$F_E = F_M + F_{\Delta\sigma} \tag{2}$$

where $F_M$ represents the magnitude scaling term, ignoring near-distance-saturation effects, and $F_{\Delta\sigma}$ represents the stress parameter scaling term. The $F_M$ term is a function of magnitude (**M**) and is defined using a hinged-quadratic functional form that follows an empirical form from data-rich regions (e.g.[3]):

$$F_M = \begin{cases} e_0 + e_1(\mathbf{M} - \mathbf{M}_\mathrm{h}) + e_2(\mathbf{M} - \mathbf{M}_\mathrm{h})^2 & \mathbf{M} \le \mathbf{M}_\mathrm{h} \\ e_0 + e_3(\mathbf{M} - \mathbf{M}_\mathrm{h}) & \mathbf{M} > \mathbf{M}_\mathrm{h} \end{cases} \tag{3}$$

where the hinge magnitude, $\mathbf{M}_\mathrm{h}$, and the model coefficients, $e_0$, $e_2$ and $e_3$, are coefficients that are specified for each oscillator frequency (see Appendix tables).

High-frequency ground-motion levels relative to low-frequency levels are controlled by the stress parameter [11]. The stress adjustment term is defined as:

$$F_{\Delta\sigma} = e_{\Delta\sigma}\ln(\Delta\sigma/100) \tag{4}$$

where $e_{\Delta\sigma}$ describes the rate of the ground-motion scaling with the stress parameter ($\Delta\sigma$). The values of $e_{\Delta\sigma}$ as determined from the simulations have a variability in magnitude and frequency that is rather complicated, and the shape of the function differs depending on whether one is upscaling or downscaling the stress parameter. The shape can be described by a polynomial:

$$e_{\Delta\sigma} = \begin{cases} s_0 + s_1\mathrm{M} + s_2\mathrm{M}^2 + s_3\mathrm{M}^3 + s_4\mathrm{M}^4 & \Delta\sigma \le 100 \text{ bar} \\ s_5 + s_6\mathrm{M} + s_7\mathrm{M}^2 + s_8\mathrm{M}^3 + s_9\mathrm{M}^4 & \Delta\sigma > 100 \text{ bar} \end{cases} \tag{5}$$

where $s_0$ to $s_9$ are frequency-dependent coefficients.

Geometrical spreading effects are modeled using an equivalent point-source distance metric:

$$R = \sqrt{{D_{rup}}^2 + h^2} \tag{6}$$

where $D_{rup}$ is the closest distance from the site to the fault-rupture surface (km) and $h$ is a pseudo-depth term that accounts for distance saturation effects. The pseudo-depth term is adopted from inversion results for active regions [17], for which there are sufficient data to constrain such effects:

$$h = 10^{\,-0.405 + 0.235\mathrm{M}} \tag{7}$$

For small to moderate events we may assume that $D_{rup}$ is equivalent to the hypocentral distance ($D_{hypo}$). The geometrical spreading function ($F_Z$) is:

$$F_Z = \ln(Z) + (b_3 + b_4 \mathrm{M}) \ln\left(R/R_{ref}\right) \quad (8)$$

where $Z$ represents the geometrical attenuation of Fourier amplitudes, whilst the multiplicative component, $(b_3 + b_4\mathbf{M}) \ln(R/R_{ref})$, accounts for the change in the apparent attenuation that occurs when ground motions are modeled in the response spectral domain rather than the Fourier domain. $R_{ref}$ is the reference effective distance, given as $R_{ref} = \sqrt{1 + h^2}$. $Z$ is a hinged bilinear model that provides for a transition from direct-wave spreading to surface-wave spreading of reflected and refracted waves:

$$Z = \begin{cases} R^{b_1} & R \le R_t \\ {R_t}^{b_1}(R/R_t)^{b_2} & R > R_t \end{cases} \quad (9)$$

where $R_t$ represents the transition distance (=50 km), and $b_1$ (=-1.3) and $b_2$ (=-0.5) are the geometrical attenuation rates of Fourier amplitudes at $R \le R_t$ and $R > R_t$, respectively.

The anelastic attenuation function ($F_\gamma$) is given as:

$$F_\gamma = \gamma D_{rup} \quad (10)$$

where $\gamma$ is a frequency-dependent anelastic attenuation coefficient. Note that the coefficients describing geometric spreading and anelastic attenuation can be determined in ENA from empirical data for small-to-moderate earthquakes.

The site effects ($F_S$) are given relative to a reference site condition, in this case hard rock (travel-time weighted average shear-wave velocity over the top 30 m, $V_{S30}$ ~2000m/s); this is the site condition corresponding to most seismograph records in eastern Canada. The approach taken in Atkinson et al. [20] was to use regression to determine site terms directly from the observations, along with the regional coefficients for attenuation.

The key attribute of the methodology behind the generic GMM is that most of the magnitude and distance scaling terms are fixed by previously-calibrated simulation studies in data-rich regions, whilst a select few parameters –specifically the average stress parameter, anelastic attenuation and calibration constant – are fine-tuned for the region of interest. In other words, we calibrate a well-behaved and validated generic model for a specific region of interest; the calibration can be accomplished using limited data on amplitude levels, site attributes, and attenuation.

The GMM developed for rock sites in eastern Canada using this method is illustrated in Figure 2 and compared to the corresponding functions for California. The comparison is made at high frequencies, for which rock amplitudes are significantly higher in ENA than in California due to a larger average value of stress parameter. At low frequencies (not shown), ENA and California amplitudes agree more closely. Note that the available data range for observations in ENA is limited, so for larger magnitudes the overall scaling behavior is effectively constrained by the underlying seismological model, which was calibrated for events in California of **M**3.0 to 7.5.

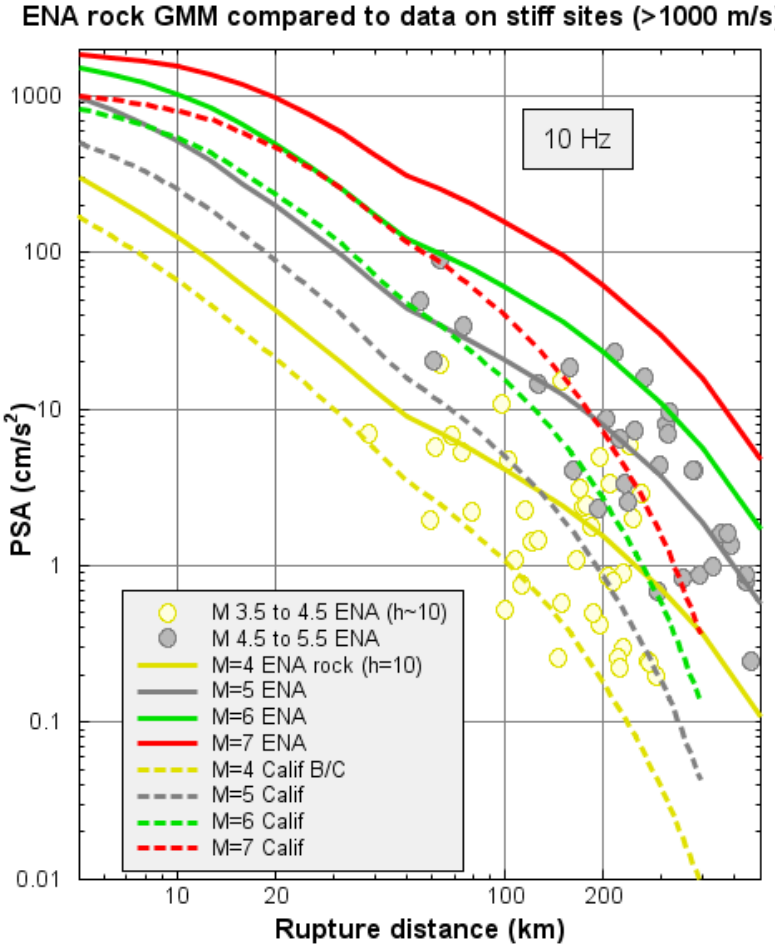


*FIG 2. ENA GMM for hard rock site conditions ($V_{S30} \approx 2000$ m/s) (solid lines) compared with eastern Canadian data recorded on stiff (Vs>1000 m/s) and rock sites (Vs~2000 m/s) (circles). California GMM for B/C sites based on the same model is shown for comparison, using dashed lines.*

Hassani and Atkinson [21] further generalized the generic GMM to enhance its usefulness for a wider range of regions and site conditions, by including a new term in the GMM to account for the effects of the near-surface attenuation parameter ($\kappa_0$) on the response spectral domain ground-motion amplitudes (PSA) as well as on the ground-motion peak amplitudes (PGA and PGV):

$$\ln \quad (Y) = F_E + F_{\kappa_0} + F_Z + F_\gamma + F_S + C \qquad (11)$$

The kappa term ($F_{\kappa_0}$) models the effects of near-surface high-frequency attenuation effects ($\kappa_0$) [22, 23] in the response spectral domain. The interplay between the stress parameter and kappa is what controls the amplitudes of ground motions at high frequencies. This interplay is illustrated in Figure 3 (see [11] for details).

The inclusion of a kappa term makes the GMM somewhat more complicated but facilitates adjustment of the $\kappa_0$ value within the modified generic GMM to model a broader range of regions and reference site conditions. For further details of the use of this form the reader is referred to [21]. Another advantage of having a $\kappa_0$ term within the GMM is the ability to invert for the $\kappa_0$ value using the response spectral amplitudes.

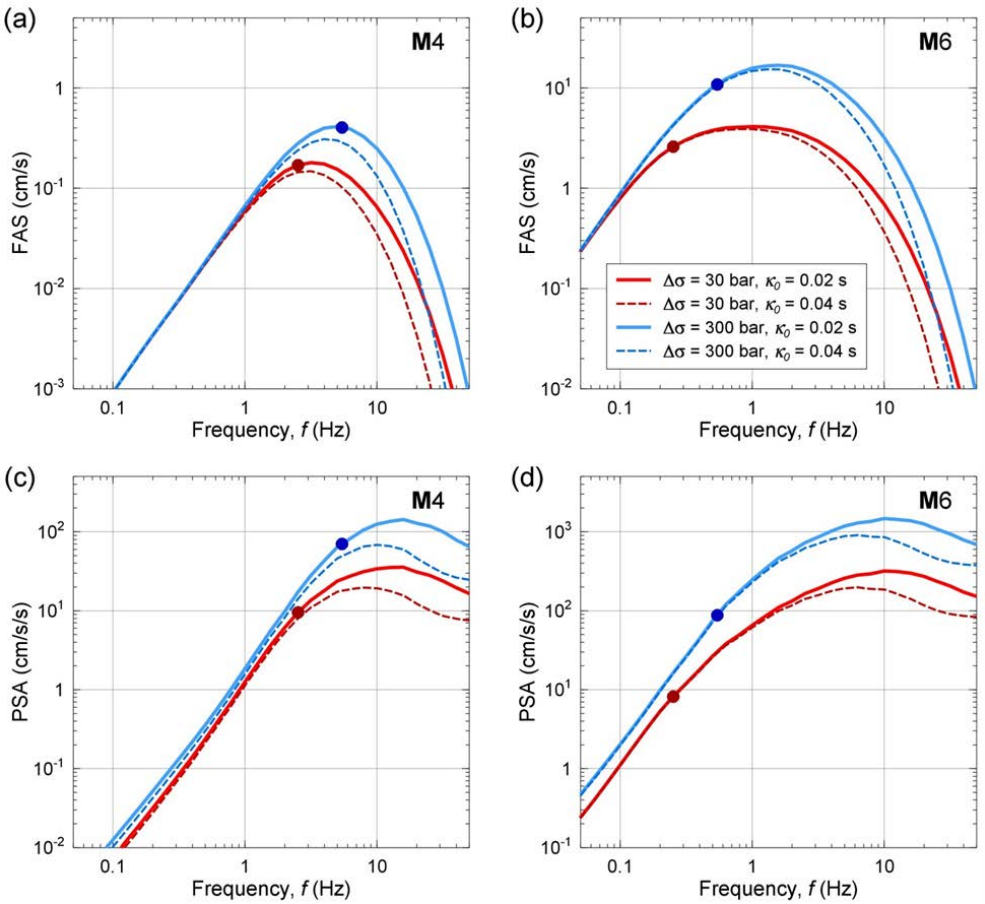


*FIG 3. Illustration of the effects of stress parameter (values of 30 bars and 300 bars are shown) and kappa (values of 0.02 s and 0.04 s are shown) on ground-motion amplitudes in the Fourier domain (a, b) and response spectral domain (c, d), for **M**=4 and M=6 at R=10 km. Dots show the corner frequency associated with the specified magnitudes and stress parameter values.*

Figure 4 shows the response spectral amplitudes at near-source distance ($D_{rup}$ = 1 km) for $\Delta\sigma$ = 100 bars and different $\kappa_0$ values, for the adjustment model of Hassani and Atkinson [21], over a wide range of magnitudes. This illustrates how maximum ground-motion amplitudes (before attenuation by path effects) are influenced by kappa in the response spectral domain. Effects can be pronounced at f>10 Hz. For example, based on calculations with the model (not shown), for an event of **M**=6 having a stress parameter of 300 bars, median 20-Hz PSA at 10 km would be ~490 cm/s$^2$ for a very hard rock site with $\kappa_0$ =0.002. This scenario is the type of event that contributes significantly to hazard for nuclear sites in ENA situated on hard rock. However, it has been suggested that kappa values on some rock sites may be significantly higher than on others. For the same scenario event at a site for which $\kappa_0$ =0.01, the median PSA would be only ~330 cm/s$^2$. Thus kappa is an important high-frequency site parameter for rock sites.

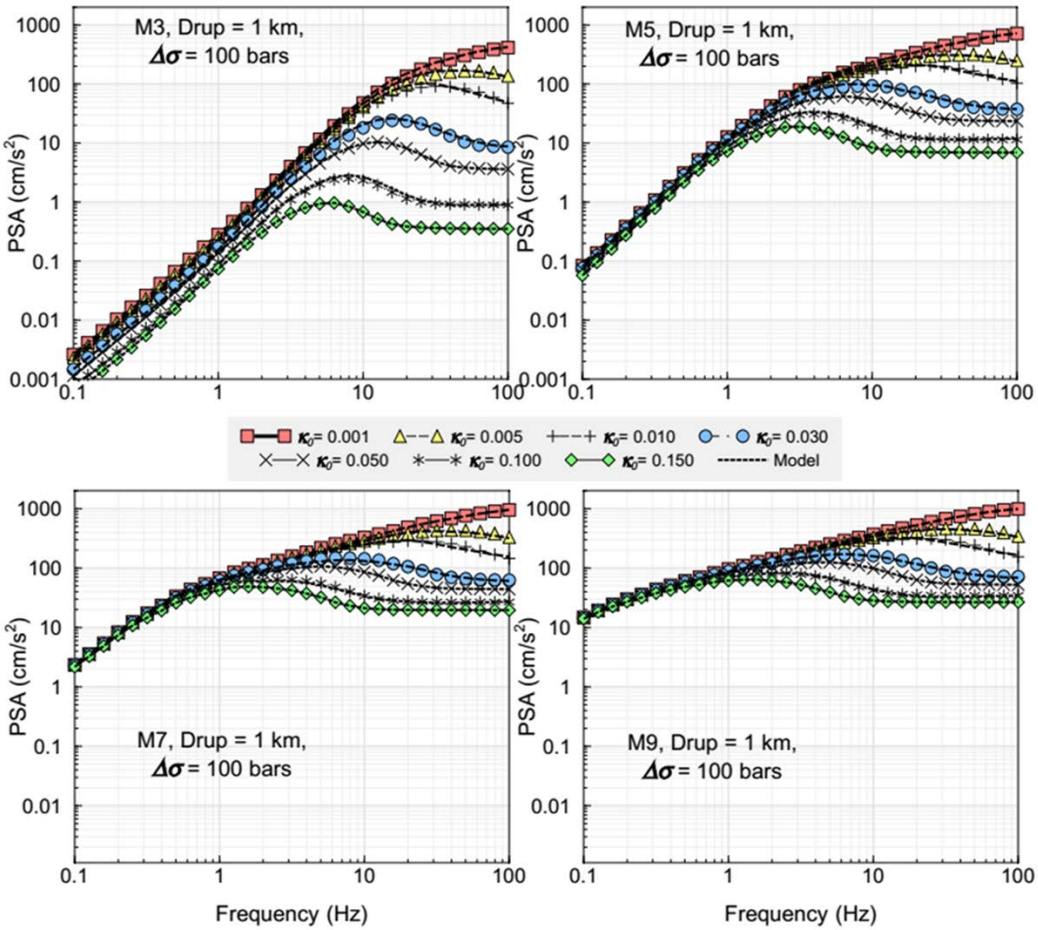


*FIG. 4. Response spectral amplitudes at 1 km for hard-rock sites from Hassani and Atkinson GMM model for **M** 3, 5, 7 and 9 for a stress parameter of 100 bars, showing influence of kappa.*

The generic GMM model as presented in the foregoing is a useful way to encapsulate simple seismological models into a convenient functional form that facilitates the modeling of key source effects (**M**, stress parameter), path effects (geometric spreading and anelastic attenuation) and site effects (near-surface amplification and kappa), without the need to repeat simulations. It can be calibrated to limited regional ground-motion observations to provide a complete and robust GMM that follows scaling constraints in magnitude-distance space as established by empirical GMMs in data-rich regions. As such, it forms a practical and effective bridge between empirical and simulation-based modeling approaches.

## 3. ALEATORY UNCERTAINTY

Seismic hazard is driven not only by median ground motions but also by their uncertainty. Uncertainty is, partly by convention, partitioned into components expressing random variability about the median (aleatory uncertainty) and uncertainty regarding the true median values (epistemic uncertainty) [24, 25]. These uncertainties imply that there is a significant probability of receiving ground motions much larger than those expressed by the median. The aleatory uncertainty can be appreciated by inspection of Figures 1 and 2, which show that motions a factor of two or more above the median are not unusual.

The aleatory uncertainty is expressed by the standard deviation of residuals (defined as the ln(observed) – ln(predicted) amplitudes), or sigma. The total sigma can be partitioned into components that express between-event variability ($\tau$) and within-event variability ($\varphi$). $\tau$ reflects the fact that some events are stronger than others due to their source attributes, such as a higher or lower stress parameter, whilst $\varphi$ reflects deviations from the median attenuation curve for a single event. $\varphi$ is sometimes further subdivided into components expressing the within-event variability component for a single station ($\varphi_{SS}$) and the site-to-site variability ($\varphi_{S2S}$); $\varphi_{S2S}$ represents the systematic deviation of the ground motion at a specific site from the median event-corrected ground motion predicted by the GMM (in which only a general site-class model is included). The reader is referred to Al Atik et al. [26] for details. Note that $\tau$ and $\varphi_{S2S}$ could both be considered largely epistemic in nature, as they represent systematic departures that may be predictable.

There is strong motivation to reduce sigma to its lowest possible values at nuclear sites, because the value of sigma significantly impacts the PSHA results. For plants that are founded on hard rock, such as those in eastern Canada and some parts of the eastern U.S., this can be accomplished by investing in seismic monitoring in the plant region, including in the plant vicinity, and focusing the GMM development on rock sites. By contrast, inappropriate modeling of site and source effects will result in an inflated value of sigma. This is illustrated in Figure 5, which was compiled using data on sigma from [27] with respect to the rock GMM model for ENA as presented in this paper; some data on sigma for rock sites in the Charlevoix regions relative to optimized GMMs [28] are also shown. When all ENA data, including both rock and soil sites, are used to compute sigma, and we model site response in the GMM using only $V_{S30}$ as a predictive variable, we attain high sigma values, about 0.8 ln units at high frequencies – which represents a factor of 2.2 in variability about the median for one standard deviation. If we improve the site model by including peak frequency of response for the site – which in ENA is a more important site variable than $V_{S30}$ - then we reduce the sigma by about 0.1 ln units at high frequencies. Most of this reduction comes from the $\varphi_{S2S}$ component for soil sites. If we consider only rock-like sites (those with $V_{S30}$>1000 m/s), and model the site response at each specific station based on the seismographic data recorded at the site, the total sigma drops to values in the range of 0.5 to 0.6 ln units, or a factor of 1.7 about the median, again due largely to reduction of $\varphi_{S2S}$. Finally, if we use a magnitude scale that reflects high-frequency amplitudes as the basis for the GMM, instead of moment magnitude, we can reduce the $\tau$ component at higher frequencies [29]. As an example, Atkinson [28] showed that total sigma for rock sites in the Charlevoix region, when modeled using Nuttli magnitude (MN), is ~0.5 ln units. Moreover, these sigma values are attained for small-to-moderate events, that typically have higher sigma than larger events, due to greater event-to-event variability in source parameters (e.g. [30]).

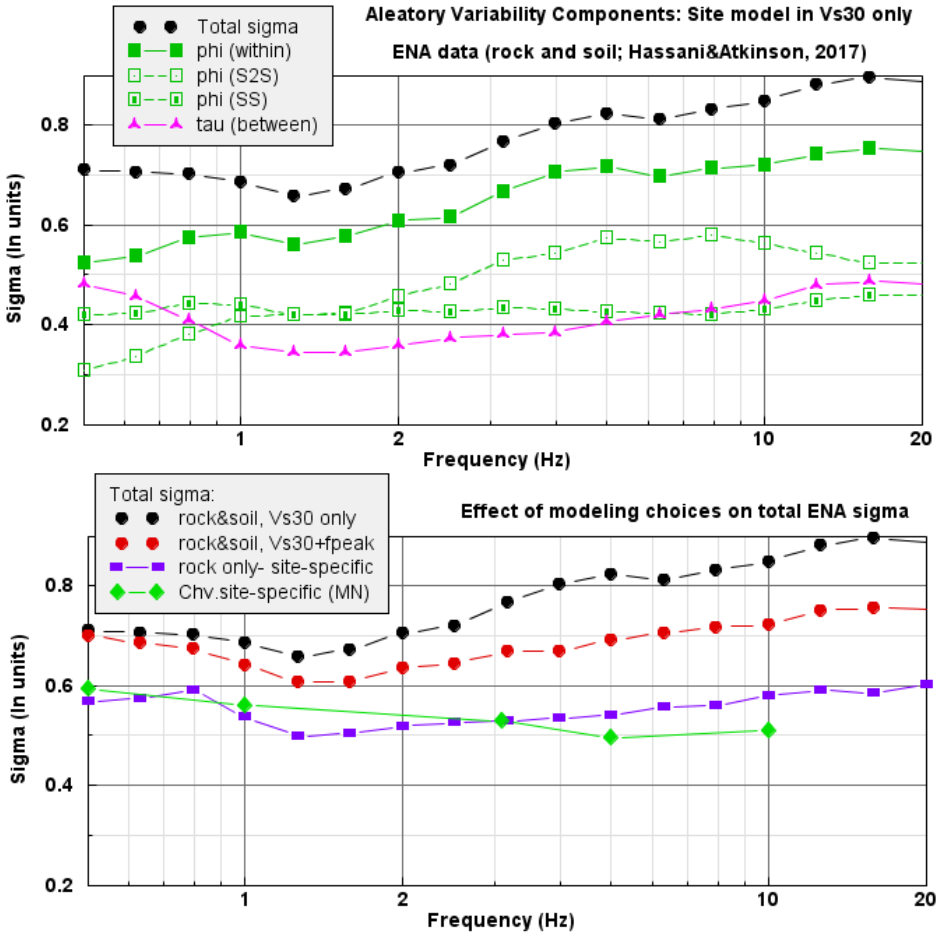


*FIG. 5. Top – Components of aleatory variability (sigma) for ENA rock and soil data (from [27]) when $V_{S30}$ is the only site variable, showing total sigma and its components (between-event τ, within-event φ and its sub-components $\varphi_{S2S}$ and $\varphi_{SS}$). Bottom – Effect of GMM site-variable modeling choices for ENA, showing sigma from [27]data if modeling rock and soil data with $V_{S30}$ only (black), with both $V_{S30}$ and fpeak (red), or using only rock data and removing site-specific response terms (purple squares). Green diamonds show sigma using site-specific GMM for Charlevoix modeled in MN (a high-frequency magnitude) (from [28]).*

The conclusion from the foregoing discussion is that sigma could be greatly reduced for nuclear sites on rock, resulting in lower calculated hazard. However, this reduction can only be achieved if high-quality seismic monitoring (e.g. broadband seismograph stations) is installed and operated over a period of years, and an investment is also made in data analysis and targeted GMM development using the data. This has not been the approach taken in most parts of ENA to date.

## 4. EPISTEMIC UNCERTAINTY

Epistemic uncertainty in median GMMs has often been modeled using alternative equations (typically those derived by various authors and approaches), with model weights in a PSHA logic tree being used to represent the relative confidence in each alternative. However, this is not necessarily the best way to model epistemic uncertainty in GMMs [ 24, 31, 32, 33]. An alternative often used in site-specific studies is to define a representative or central-branch GMM, along with upper and lower variants that express uncertainty about the central model.

This approach offers more flexibility in expressing uncertainty in knowledge of the correct median GMM. The representative equation approach also has significant practical utility, enabling a complex problem to be represented by a minimum number of branches for hazard calculations, which is efficient and transparent. A drawback is that a significant degree of judgment need be exercised regarding the selection of the central model and its upper and lower branches. However, such subjective judgments are equally important when using the alternative-GMM approach, as the selection and weighting of alternative models is also a process based on subjective judgment. To get around the drawbacks of both the representative suite and alternative GMM approaches, a more sophisticated and objective approach to representing model alternatives, based on Sammon's mapping of predicted amplitudes in higher-order dimensions, has been used in some projects, such as the NGA-East project [30]. This is a powerful approach but not easy to implement or adjust on a site-specific basis as more information is obtained.

To some extent, the details of the method used to represent epistemic uncertainty may not be of critical importance. Sensitivity tests indicate that it is the range covered by the GMM models and their relative weights that are important to the PSHA results, not the mechanics of how they are treated [32]. An additional consideration is that the division of ground-motion uncertainty into its epistemic and aleatory components is ambiguous and non-unique, because some factors of the total uncertainty could be cast into either component [25]. In contemplating the epistemic versus aleatory subdivision, a factor to consider is that whilst GMMs cover a range of possible magnitude-distance scenarios, the actual "design event" that an individual structure may be required to withstand is really a single future event having specific source, path and site attributes, at some sigma level. This is because large potentially-damaging earthquakes are rare events, and most structures will be expected to withstand only one such event in their design life. Moreover, for a nuclear plant there would be inspection and repair immediately following any strong event and a re-set of the facility's capacity. We don't know in advance the specifics of this event. But we can model this uncertainty within the context of PSHA in a few ways. The simplest, assuming we also wish to use site-targeted aleatory uncertainty as described in the previous section, is to use the representative suite approach to define the epistemic uncertainty about the central branch GMM. In concept, all inter-event components of uncertainty (most of the $\tau$ component of aleatory variability) could be modeled as epistemic, whilst the aleatory uncertainty then represents just the variability of observations about the median event-specific prediction equation for a single station (ie. $\varphi_{SS}$). Considering the variability components of Figure 5, the appropriate modeling of epistemic uncertainty might reduce the aleatory component to the range of 0.4 to 0.5 ln units.

Such an approach presupposes that we can model epistemic uncertainty in ground motions from future events through definition of the distribution of earthquake source, path and site parameters of the GMM model. The generic GMM approach outlined here is a practical way to implement such distributions in Monte Carlo PSHA software, in which simulated earthquake catalogues and their generated ground motions at a site are used to calculate the ground-motion distribution at a site [34, 35]. For each simulated earthquake magnitude and location, we would draw (by Monte Carlo, from a defined distribution) a value of stress parameter and a value of attenuation (frequency-dependent, including geometric spreading and anelastic effects). The aleatory uncertainty for calculations at a specified site (with known response characteristics from network observations) would be that attributable to $\varphi_{SS}$. This approach would allow PSHA to be more site-specific in its application of epistemic and aleatory uncertainties.

## 5. CONCLUDING REMARKS

This paper has dealt with the use of conventional GMMs to define ground motion and its epistemic and aleatory uncertainty, within the context of contemporary PSHA methodology. In the longer term, a truly site-specific PHSA would be based on simulations that fully consider the source, path and site attributes that govern ground motions for all potential future earthquake scenarios, eliminating the need for GMMs altogether (e.g. [36]). However, such an approach will require substantial further improvement of our knowledge of earthquake source, path and site processes. Until such advances can be achieved, the use of GMMs that bridge seismological and empirical approaches are an effective tool to represent the distribution of ground motion and its uncertainty in seismic hazard assessment.

## 6. REFERENCES

[1 ] Bozorgnia, Y., N.A. Abrahamson, L.A. Atik, T.D. Ancheta, G.M. Atkinson, J.W. Baker, A. Baltay, D.M. Boore, K.W. Campbell, B.S.-J. Chiou, R. Darragh, S. Day, J. Donahue, R.W. Graves, N. Gregor, T. Hanks, I.M. Idriss, R. Kamai, T. Kishida, A.R. Kottke, S.A. Mahin, S. Rezaeian, B. Rowshandel, E. Seyhan, S. Shahi, T. Shantz, W. Silva, P. Spudich, J.P. Stewart, J. Watson-Lampery, K. Wooddell, and R. Youngs (2014). NGA-West2 research project, Earthquake Spectra, **30,** 973-987.

[2] Abrahamson, N.A., W.J. Silva, and R. Kamai (2014). Summary of the ASK14 ground motion relation for active crustal regions, Earthquake Spectra. **30** 1025-1055.

[3] Boore, D.M., J.P. Stewart, E. Seyhan, and G.M. Atkinson (2014). NGA-West2 equations for predicting PGA, PGV, and 5% damped PSA for shallow crustal earthquakes, Earthquake Spectra, **30,** 1057-1085.

[4] Campbell, K.W., and Y. Bozorgnia (2014). NGA-West2 ground motion model for the average horizontal components of PGA, PGV, and 5% damped linear acceleration response spectra, Earthquake Spectra, **30,** 1087-1115.

[5] Chiou, B.S.-J., and R.R. Youngs (2014). Update of the Chiou and Youngs NGA model for the average horizontal component of peak ground motion and response spectra, Earthquake Spectra, **30,** 1117-1153.

[6] Idriss, I. (2014). An NGA-West2 empirical model for estimating the horizontal spectral values generated by shallow crustal earthquakes, Earthquake Spectra, **30,** 1155-1177.

[7] Petersen, M.D., M.P. Moschetti, P.M. Powers, C.S. Mueller, K.M. Haller, A.D. Frankel, Y. Zeng, S. Rezaeian, S.C. Harmsen, and O.S. Boyd (2015). The 2014 United States national seismic hazard model, Earthquake Spectra, **31,** S1-S30.

[8] Boore, D.M. (1983). Stochastic simulation of high-frequency ground motions based on seismological models of the radiated spectra, Bull. Seism. Soc. Am.,**73,** 1865-1894.

[9] Atkinson, G.M., and D.M. Boore (1995). Ground-motion relations for eastern North America, Bull. Seism. Soc. Am., **85,** 17-30.

[10] Toro, G.R., N.A. Abrahamson, and J.F. Schneider (1997). Model of strong ground motions from earthquakes in central and eastern North America: best estimates and uncertainties, Seism. Res. L., **68,** 41-57.

[11] Boore, D.M. (2003). Simulation of ground motion using the stochastic method, Pure and applied geophysics, **160,** 635-676.

[12] Beresnev, I. and G. Atkinson (1997). Modeling finite fault radiation from the $w^n$ spectrum. Bull. Seism. Soc. Am., **87**, 67-84.

[13] Motazedian, D., and G.M. Atkinson (2005). Stochastic finite-fault modeling based on a dynamic corner frequency, Bull. Seism. Soc. Am., **95,** 995-1010.

[14] Assatourians, K., and G. Atkinson (2007). Modeling variable stress drop with the stochastic finite-fault model. Bull. Seism. Soc. Am., **97**, 1935-1949.

[15] Frankel, A. (2009). A constant stress-drop model for producing broadband synthetic seismograms: Comparison with the Next Generation Attenuation relations, Bull. Seism. Soc. Am., **99,** 664-680.

[16] Frankel, A.D. (2015). Ground-Motion Predictions for Eastern North American Earthquakes Using Hybrid Broadband Seismograms from Finite-Fault Simulations with Constant Stress-Drop Scaling in *NGA-East: Median Ground-Motion Models for the Central and Eastern North America Region*, Chap. 6, PEER Report No. 2015/04, Pacific Earthquake Engineering Research Center, Berkeley, CA, 149-163.

[17] Yenier, E., and G.M. Atkinson (2015). An equivalent point-source model for stochastic simulation of earthquake ground motions in California, Bull. Seism. Soc. Am., **105** 1435-1455.

[18] Yenier, E., and G.M. Atkinson (2015). Regionally adjustable generic ground-motion prediction equation based on equivalent point-source simulations: Application to central and eastern North America, Bull. Seism. Soc. Am., **105,** 1989-2009.

[19] Seyhan, E., and J.P. Stewart (2014). Semi-empirical nonlinear site amplification from NGA-West2 data and simulations, Earthquake Spectra, **30,** 1241-1256.

[20] Atkinson, G., B. Hassani, A.Singh, E. Yenier and K. Assatourians (2015). Estimation of moment magnitude and stress parameter from ShakeMap ground-motions. Bull. Seism. Soc. Am., **105**, 2572-2588.

[21] Hassani, B. and G. Atkinson (2018). Adjustable Generic Ground-Motion Prediction Equation Based on Equivalent Point-Source Simulations: Accounting for Kappa Effects. Bull. Seism. Soc. Am., in press.

[22] Anderson, J.G., and S.E. Hough (1984). A model for the shape of the Fourier amplitude spectrum of acceleration at high frequencies, Bull. Seism. Soc. Am., **74,** 1969-1993.

[23] Van Houtte, C., S. Drouet, and F. Cotton (2011). Analysis of the origins of κ (kappa) to compute hard rock to rock adjustment factors for GMMs, Bull. Seism. Soc. Am., **101,** 2926-2941.

[24] Bommer, J. and F. Scherbaum (2008). The use and misuse of logic trees in probabilistic seismic hazard analysis. Earthquake Spectra, **24**, 997-1009.

[25] Strasser, F., N. Abrahamson and J. Bommer (2009). Sigma: Issues, insights and challenges. Seism. Res. L., **80**, 40-56.

[26] Al Atik, L., Abrahamson, N.A., Bommer, J.J., Scherbaum, F., Cotton, F., and Kuehn, N. (2010). The variability of ground-motion prediction models and its components. Seism. Res. L., **81**, 794−801.

[27] Hassani, B., and G.M. Atkinson (2017). Site-Effects Model for Central and Eastern North America Based on Peak Frequency and Average Shear Wave Velocity, Bull. Seism. Soc. Am., **107**, doi: 10.1785/0120170062.

[28] Atkinson, G. (2013). Empirical evaluation of aleatory and epistemic uncertainty in eastern ground motions. Seism. Res. L., **84**, 130-138.

[29] Atkinson, G. (1995). Optimal choice of magnitude scales for seismic hazard analysis. Seism. Res. L., **66**, 51-55.

[30] Goulet, C., Y. Bozognia, N. Abrahamson, N. Kuehn, L. Al Atik, R. Youngs, R. Graves and G. Atkinson (2017). NGA-East Models for the U.S. Geological National Survey Seismic Hazard Maps. PEER Report 2017-03. Pacific Earthquake Engineering Research Center, University of California, Berkeley. March 2017.

[31] Atkinson, G. (2011). An empirical perspective on uncertainty in earthquake ground motions. Can.J.Civil Eng., **38**,1-14. DOI:10.1139/l10-120.

[32] Atkinson, G. and J. Adams (2013). Ground motion prediction equations for application to the 2015 national seismic hazard maps of Canada. Can. J. Civil Eng., **40**, 988-998.

[33] Atkinson, G., J. Bommer and N. Abrahamson (2014). Alternative approaches to modeling epistemic uncertainty in ground motions in Probabilistic Seismic Hazard Analysis. Seism. Res. L., **85**, 1-3.

[34] Musson, R. M. W. (1999). Determination of design earthquakes in seismic hazard analysis through Monte Carlo simulation, J.Earthquake Eng.**, 3,** 463-474.

[35] Assatourians, K. and G. Atkinson (2013). EqHaz – An open-source probabilistic seismic hazard code based on the Monte-Carlo simulation approach. Seism. Res. L., **84**, 516-524.

[36] Atkinson, G. (2012). Integrating advances in seismic hazard and ground motion analysis. Proc. 15th World Conf. Earthq.Eng., Lisbon, Sept. 2012.

## APPENDIX: Coefficient Tables for ENA Rock GMM of Atkinson et al., 2015

| freq (Hz) | C | Mh | e0 | e1 | e2 | e3 | b3 | b4 | γ |
|---|---|---|---|---|---|---|---|---|---|
| 0.10 | -0.250 | 7.45 | -0.2763 | 1.9720 | -0.0463 | 1.7230 | -0.6196 | 0.08420 | -0.00130 |
| 0.20 | -0.250 | 6.85 | -0.0792 | 1.9800 | -0.0621 | 1.5850 | -0.5800 | 0.07896 | -0.00130 |
| 0.33 | -0.250 | 6.65 | 0.5156 | 1.9080 | -0.0898 | 1.4180 | -0.5129 | 0.06761 | -0.00130 |
| 0.50 | -0.250 | 6.65 | 1.2510 | 1.7480 | -0.1316 | 1.1920 | -0.4353 | 0.05361 | -0.00130 |
| 0.63 | -0.445 | 6.75 | 1.7530 | 1.5640 | -0.1678 | 1.0540 | -0.3849 | 0.04430 | -0.00130 |
| 0.77 | -0.605 | 6.75 | 2.0110 | 1.3860 | -0.2057 | 1.0000 | -0.3503 | 0.03777 | -0.00130 |
| 1.00 | -0.770 | 6.45 | 1.9860 | 1.3400 | -0.2456 | 0.9829 | -0.2974 | 0.02765 | -0.00130 |
| 1.25 | -0.878 | 6.85 | 2.6640 | 0.9053 | -0.2888 | 0.8944 | -0.2523 | 0.01906 | -0.00130 |
| 1.54 | -0.951 | 6.60 | 2.6170 | 0.8758 | -0.3160 | 0.9251 | -0.2277 | 0.01371 | -0.00130 |
| 2.00 | -1.007 | 6.25 | 2.5440 | 0.8856 | -0.3486 | 0.9182 | -0.2079 | 0.00854 | -0.00130 |
| 2.50 | -1.022 | 6.15 | 2.6740 | 0.8501 | -0.3469 | 0.8966 | -0.1927 | 0.00485 | -0.00173 |
| 3.33 | -0.997 | 5.85 | 2.6350 | 0.8471 | -0.3631 | 0.8763 | -0.2117 | 0.00516 | -0.00231 |
| 4.00 | -0.956 | 5.60 | 2.5170 | 0.8671 | -0.3775 | 0.8785 | -0.2429 | 0.00921 | -0.00267 |
| 5.00 | -0.878 | 5.45 | 2.5490 | 0.8194 | -0.3860 | 0.8426 | -0.2868 | 0.01376 | -0.00312 |
| 6.25 | -0.770 | 5.25 | 2.4660 | 0.8088 | -0.3871 | 0.8407 | -0.3265 | 0.01918 | -0.00357 |

| | | | | | | | | | |
|---|---|---|---|---|---|---|---|---|---|
| 7.69 | -0.643 | 5.35 | 2.6410 | 0.7346 | -0.3321 | 0.8116 | -0.3551 | 0.02224 | -0.00398 |
| 10.0 | -0.600 | 5.45 | 2.7770 | 0.7118 | -0.2619 | 0.7941 | -0.3774 | 0.02472 | -0.00451 |
| 12.5 | -0.600 | 5.20 | 2.5760 | 0.7651 | -0.2434 | 0.7865 | -0.4210 | 0.03071 | -0.00495 |
| 15.4 | -0.600 | 5.75 | 2.9970 | 0.6842 | -0.1547 | 0.7553 | -0.4665 | 0.03640 | -0.00537 |
| 20.0 | -0.600 | 5.35 | 2.5590 | 0.7193 | -0.1636 | 0.7545 | -0.5096 | 0.04279 | -0.00550 |
| 50.0 | -0.600 | 5.90 | 2.3780 | 0.6999 | -0.1066 | 0.7488 | -0.6377 | 0.06251 | -0.00550 |
| PGA | -0.380 | 5.85 | 2.2160 | 0.6859 | -0.1392 | 0.7656 | -0.6187 | 0.06029 | -0.00490 |
| PGV | -0.740 | 5.90 | 5.9600 | 1.0300 | -0.1651 | 1.0790 | -0.5785 | 0.05737 | -0.00290 |

| freq (Hz) | s0 | s1 | s2 | s3 | s4 | s5 | s6 | s7 | s8 | s9 |
|---|---|---|---|---|---|---|---|---|---|---|
| 0.10 | -2.1940 | 1.5110 | -0.2871 | 0.01534 | 0.00024 | 0.2684 | -0.3862 | 0.2169 | -0.03967 | 0.00230 |
| 0.20 | -6.3880 | 5.0830 | -1.3810 | 0.15760 | -0.00636 | -1.3770 | 0.9093 | -0.1422 | 0.00132 | 0.00071 |
| 0.33 | -7.9800 | 6.6430 | -1.9240 | 0.23660 | -0.01039 | -4.1800 | 3.3170 | -0.8862 | 0.09888 | -0.00385 |
| 0.50 | -6.6420 | 5.7670 | -1.7420 | 0.22410 | -0.01028 | -6.0100 | 4.9850 | -1.4330 | 0.17480 | -0.00759 |
| 0.63 | -5.2640 | 4.7380 | -1.4760 | 0.19630 | -0.00928 | -5.8800 | 4.9780 | -1.4650 | 0.18320 | -0.00816 |
| 0.77 | -2.5080 | 2.5230 | -0.8446 | 0.12050 | -0.00602 | -5.4940 | 4.7660 | -1.4390 | 0.18490 | -0.00846 |
| 1.00 | 1.0660 | -0.4552 | 0.0374 | 0.01033 | -0.00108 | -4.4730 | 4.0510 | -1.2740 | 0.17100 | -0.00814 |
| 1.25 | 2.4040 | -1.6520 | 0.4088 | -0.03710 | 0.00105 | -2.1240 | 2.1520 | -0.7301 | 0.10530 | -0.00529 |
| 1.54 | 3.6450 | -2.8220 | 0.7932 | -0.08926 | 0.00356 | -0.6671 | 0.9277 | -0.3708 | 0.06183 | -0.00343 |
| 2.00 | 3.9560 | -3.2880 | 0.9885 | -0.11960 | 0.00514 | 0.8555 | -0.4528 | 0.0646 | 0.00522 | -0.00083 |
| 2.50 | 2.0180 | -1.8570 | 0.6117 | -0.07674 | 0.00334 | 2.4220 | -1.9380 | 0.5558 | -0.06174 | 0.00239 |
| 3.33 | -0.3182 | -0.1386 | 0.1704 | -0.02850 | 0.00142 | 2.2450 | -2.0030 | 0.6326 | -0.07699 | 0.00327 |
| 4.00 | -1.7670 | 0.9826 | -0.1314 | 0.00600 | -0.00001 | 1.7800 | -1.7670 | 0.6066 | -0.07834 | 0.00350 |
| 5.00 | -2.7070 | 1.7290 | -0.3302 | 0.02816 | -0.00091 | 0.8197 | -1.0830 | 0.4395 | -0.06105 | 0.00285 |
| 6.25 | -3.9650 | 2.8200 | -0.6499 | 0.06720 | -0.00261 | -0.1997 | -0.3370 | 0.2570 | -0.04252 | 0.00218 |
| 7.69 | -4.1740 | 3.0920 | -0.7438 | 0.07982 | -0.00321 | -1.3840 | 0.6264 | -0.0116 | -0.01092 | 0.00083 |
| 10.0 | -4.0510 | 3.1000 | -0.7625 | 0.08328 | -0.00339 | -2.4520 | 1.5690 | -0.2890 | 0.02300 | -0.00066 |
| 12.5 | -3.6850 | 2.9620 | -0.7510 | 0.08421 | -0.00351 | -3.1390 | 2.1770 | -0.4674 | 0.04466 | -0.00160 |
| 15.4 | -2.2250 | 1.9480 | -0.4900 | 0.05486 | -0.00229 | -3.9600 | 2.8710 | -0.6675 | 0.06883 | -0.00265 |
| 20.0 | -0.9628 | 0.9826 | -0.2156 | 0.02080 | -0.00074 | -4.2280 | 3.2930 | -0.8316 | 0.09303 | -0.00387 |
| 50.0 | -1.1600 | 1.2740 | -0.3344 | 0.03911 | -0.00170 | -1.2720 | 1.2540 | -0.3171 | 0.03624 | -0.00155 |
| PGA | -2.1320 | 1.9370 | -0.5040 | 0.05824 | -0.00250 | -1.4440 | 1.2350 | -0.2851 | 0.03021 | -0.00122 |
| PGV | -2.2460 | 1.9510 | -0.5181 | 0.06139 | -0.00273 | -1.7580 | 1.3790 | -0.3256 | 0.03500 | -0.00143 |